AIAA AVIATION Forum
12-16 June 2023, San Diego, CA and Online
AIAA AVIATION 2023 Forum

10.2514/6.2023-4276

Check for updates

Utilization of Pulsed Electrothermal Heating for Aircraft Icing Mitigation

Kiran Digavalli[1], Harsha Sista[2], Chukwudum Eluchie[3], Haiyang Hu[4], Hui Hu[5]
Iowa State University, Ames, IA, 50011, USA

Ice accretion on aerodynamic surfaces is both a serious threat to aircraft safety, and a severe detriment to wind turbine power output. The accretion of ice structures on aircraft wings and wind turbine blades alters their shape, thus causing a decrease in lift and an increase in drag. Passive anti/de-icing measures constitute coatings applied to aerodynamic surfaces, which decrease the water's ability to cling to the surface, while active anti-/de-icing methods involve heating the aerodynamic surface.

A comparative study is conducted to investigate the dynamic anti-/de-icing process and unsteady heat transfer characteristics of various electric thermal methods. While an electrothermal film heater was wrapped around the leading edge of an airfoil model installed inside the icing research tunnel of Iowa State University (ISU-IRT), the effects of the applied electric voltage, duration, and frequency of the pulsed electrothermal heating on the effectiveness of the anti-/de-icing operation were evaluated under different icing conditions. The application of pulsed electrothermal heating showed clear advantages in both anti-icing and de-icing performance over continuous DC electrothermal heating at matched average power. In anti-icing, the pulse-heated model maintained an ice-free leading edge, while the continuously heated model did not. In de-icing, the pulse-heated model achieved an ice-free condition in significantly shorter time than the continuously heated model.

Downloaded by Iowa State University on July 18, 2024 | http://arc.aiaa.org | DOI: 10.2514/6.2023-4276

I. Nomenclature

$\boldsymbol{U_\infty}$ = Freestream velocity

$\boldsymbol{T_\infty}$ = Freestream temperature

$\boldsymbol{LWC}$ = Liquid Water Content

$\boldsymbol{\Delta T}$ = Temperature relative to freestream

$\boldsymbol{t_{on}}$ = DC pulsed waveform on-time

$\boldsymbol{t_{off}}$ = DC pulsed waveform off-time

$\boldsymbol{V_{peak}}$ = DC pulsed waveform peak voltage

II. Introduction

Icing on aerodynamic surfaces is both a serious threat to aircraft safety, and a severe detriment to wind turbine power output. The accretion of ice on wings and wind turbine blades alters their shape, thus causing a decrease in lift and increase in drag. In severe cases, this change can be such that an aircraft loses lift entirely, or a wind turbine no longer produces any power. There are broadly two types of ice accretion which occur on aerodynamic surfaces. Glaze ice occurs at warmer temperatures and higher liquid water contents. In glaze ice conditions, water droplets impinge

[1] Graduate Student, Department of Aerospace Engineering.
[2] Graduate Student, Department of Aerospace Engineering.
[3] Graduate Student, Department of Aerospace Engineering..
[4] Postdoctoral Research Associate, Department of Aerospace Engineering.
[5] Martin C. Jischke Professor, Dept of Aerospace Engineering, AIAA Associate Fellow. Email: huhui@iastate.edu

Copyright © 2023 by Kiran Digavalli, Harsha Sista, Chukwudum Eluchie, Haiyang Hu, Hui Hu.
Published by the American Institute of Aeronautics and Astronautics, Inc., with permission.

onto an aerodynamic surface, and subsequently distort and run back some distance before freezing [1]. Rime ice, however, occurs at lower temperatures and lower liquid water contents. The process of rime ice accretion involves no distortion or runback of the water drop after impingement upon the aerodynamic surface. Rather, rime ice accretion entails the water drop freezing immediately upon their impingement on the aerodynamic surface [1]. A hybrid glaze-rime ice accretion may occur in certain circumstances.

Methods of anti-/de-icing are divided into two categories. Passive anti/de-icing measures constitute coatings applied to aerodynamic surface, which decrease the water's ability to cling to the surface. The water, therefore, runs back over the surface faster and has less opportunity to freeze onto the surface [2]. These coatings are referred to as superhydrophobic or ice phobic coatings. They operate by increasing the contact angle of a water droplet on the surface. The contact angle is a measure of the water droplet's adhesion to the surface, and is related to the surface energy of the substrate [2]. Meanwhile, active anti-/de-icing methods include mechanical methods, whereby a rubber boot encompassing compassing the aerodynamic surface is inflated in flight, so as to break away any accumulated ice, and thermal methods which involve heating the aerodynamic surface. Aerodynamics surfaces may be heated using electrothermal methods, or using hot air bled from the aircraft compressor. However, both of these methods incur considerable power loss on the aircraft or wind turbine in question. Tian et. al. report that compressor bleed air can reduce the power output of aircraft jet engines by up to 5% [3]. Furthermore, de-icing the entire surface of a wind turbine blade using electrothermal heating may consume 70% of the power produced by the wind turbine. Miljkovic et. al. developed a method in which short pulse of heat is used to melt only the interfacial layer of ice or frost adhering to the substrate. The melted layer acts as a lubricating film, allowing gravity or gas shear to remove the remaining ice [4].

III. Experimental Setup and Process

The objectives of the present study are to characterize the temperature behavior of pulsed electrothermal heating, to examine and characterize the performance of pulsed electrothermal heating as compared to continuous heating in airfoil anti-icing and de-icing situations, and thus to draw conclusions about the use of pulsed electrothermal heating for aviation applications.

A. Pulsed DC Waveform Overview

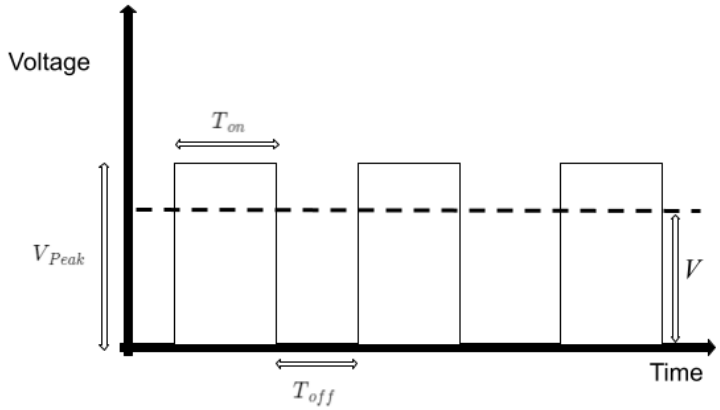

Fig. 1: Key properties of a pulsed DC waveform

In the context of this study, pulsed DC current refers to waveform which instantaneously ascends from 0 Volts to a peak voltage V_{peak}, dwells for some time T_{on}, descends instantaneously to 0 Volts, and dwells for time T_{off}, with the cycle repeating indefinitely. Key properties include duty cycle, frequency, and average power, which are calculated as follows:

$$\boldsymbol{Duty\ Cycle} = \frac{\boldsymbol{T_{on}}}{\boldsymbol{T_{on}} + \boldsymbol{T_{off}}} \tag{1}$$

$$\boldsymbol{Frequency} = \frac{\boldsymbol{1}}{\boldsymbol{T_{on}} + \boldsymbol{T_{off}}} \tag{2}$$

$$\boldsymbol{Avg.\ Power} = \frac{\boldsymbol{V_{peak}}^2}{\boldsymbol{R}} * (Duty\ Cycle) \tag{3}$$

Downloaded by Iowa State University on July 18, 2024 | http://arc.aiaa.org | DOI: 10.2514/6.2023-4276

B. Experimental Investigation to Determine the Effect of Pulse Frequency on Temperature

In order to examine the effect of pulse frequency on temperature, a preliminary experiment was carried out with electrothermal heating film was utilized in the experiment, 9.5 cm by 5 cm in size. The film was bordered by conductive busses on the two shorter sides. The resistance between the busses was 168 Ohms. The film was coated with an enamel substance to minimize infrared reflection. The film was attached by means of a spray adhesive to a piece of plywood positioned vertically on a stand. Copper leads were affixed to the conductive busses. The output cables of a digital power supply capable of supplying continuous and pulsed DC current at up to 150 Volts and 5 Amperes were connected to the copper leads. An FLIR infrared camera was placed at a distance of 40 centimeters from the surface of the resistive film, and was connected via ethernet to a computer. The FLIR camera software was used for data acquisition.

C. Experimental Investigation to Elucidate the Anti-/De-Icing Performance of Pulsed and Continuous DC Electrothermal Heating

A Kapton RS resistive heating film with a resistance of 88 Ohms was installed on NACA 0012 airfoil with a chord length of 15 cm. The film covered 30% of the area of the airfoil surface from the leading edge rearwards, on both the top and bottom surfaces. The resistive heating film was supplied with power by a DC power supply. The airfoil was placed in the Iowa State University Icing Research Tunnel, a closed-loop subsonic wind tunnel, incorporating a refrigeration system to produce freezing temperatures, and an arrangement of 9 spray nozzles which inject a mist of water into the freestream.

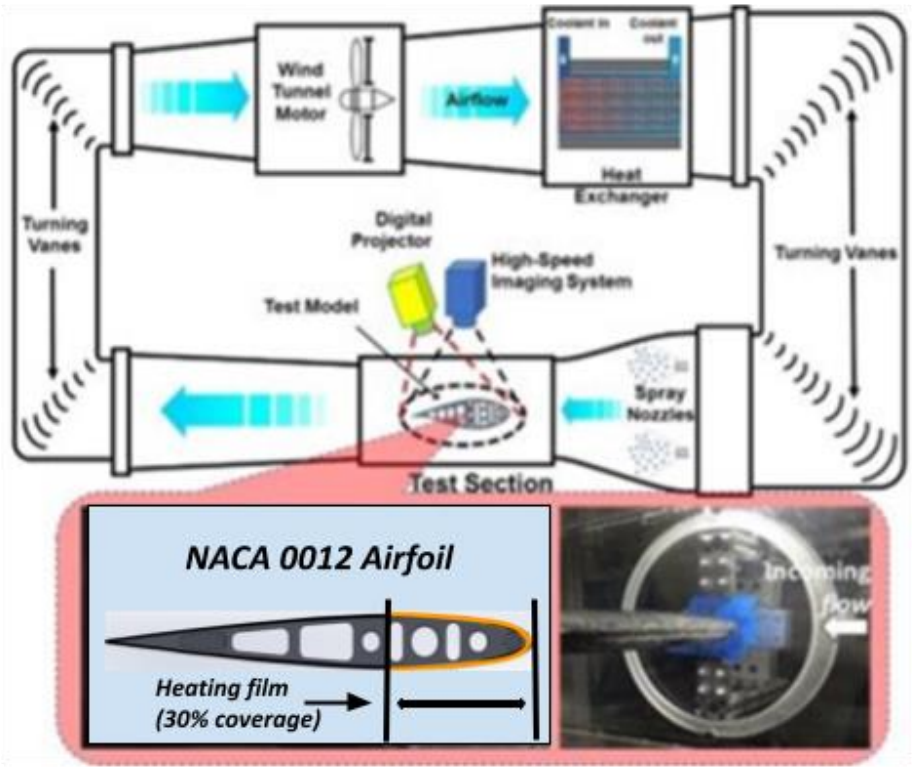

Fig. 2: A diagram of the Iowa State University Icing Research Tunnel

The pulsed current supplied to the airfoil's resistive heating film had a duty cycle of 50%, and a frequency of 0.1 Hz. V_{peak} was 150V for de-icing, and 120V for anti-icing. This corresponds to a power densities of 14.1 and 9.0 Kilowatts per Square meter, respectively. To match the average power of the pulsed current, a continuous DC voltage of 85 Volts was used for the anti-icing case, and 106V for the de-icing case. The icing tunnel was operated at a U_∞ of 40 m/s, LWC 1.0 g/m^3, and T_∞ of -5 degrees Celsius, which constitute glaze ice conditions. A Photron Fastcam high-

Downloaded by Iowa State University on July 18, 2024 | http://arc.aiaa.org | DOI: 10.2514/6.2023-4276

speed camera was positioned directly above the airfoil during tested to obtain high-speed footage of the anti-icing and de-icing behaviour. Thermocouples at the leading edge, 10% chord, 25% chord, and 50% chord were used to obtain temperature data for the airfoil, while a thermocouple placed in the freestream was used to measure T_∞. ΔT was obtained by subtracting T_∞ from the measured temperature.

Anti-icing performance was evaluated by allowing the airfoil to heat for one minute before switching the spray nozzles on, and collecting both high-speed video and infrared imaging data for 160 seconds. De-icing performance was evaluated by allowing ice to accrete on the airfoil for one and a half minutes with no heating, then switching off the spray nozzles, and switching on the heating power supply. Video and thermocouple data were collected until the heated part of the airfoil was ice-free.

IV. Results and Discussion

A. Pulsed Heating at Various Frequencies

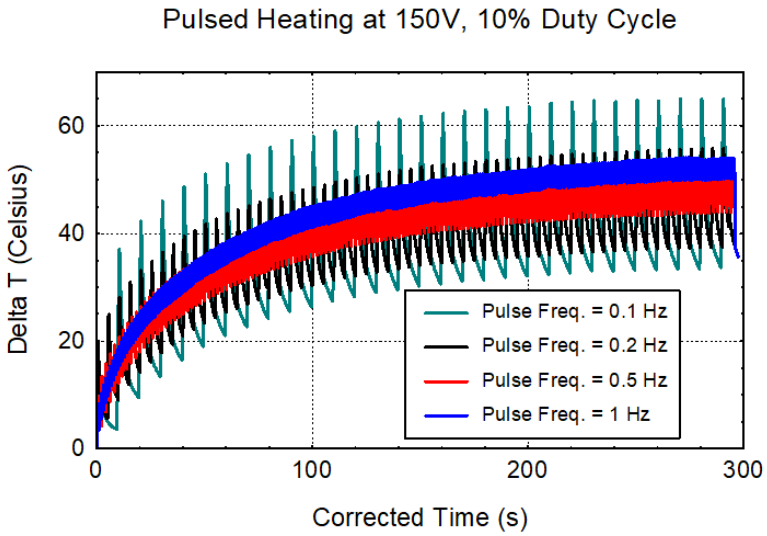

Fig. 3: Graph of temperature against time for 150V, 10% duty cycle pulsed heating with frequencies of were 1 Hz, 0.5 Hz, 0.2 Hz, and 0.1 Hz, respectively.

Fig. 3 illustrates that, while all pulse frequencies display similar average temperatures, and indeed while the graph for 1 Hz shows a slightly higher average temperature than the other frequencies, the highest peak temperatures by a considerable margin are achieved by the lowest pulse frequency, 0.1 Hz. Therefore, this pulse frequency was selected for use in the next phase of the experiment.

Downloaded by Iowa State University on July 18, 2024 | http://arc.aiaa.org | DOI: 10.2514/6.2023-4276

B. Continuous and Pulsed Anti-Icing

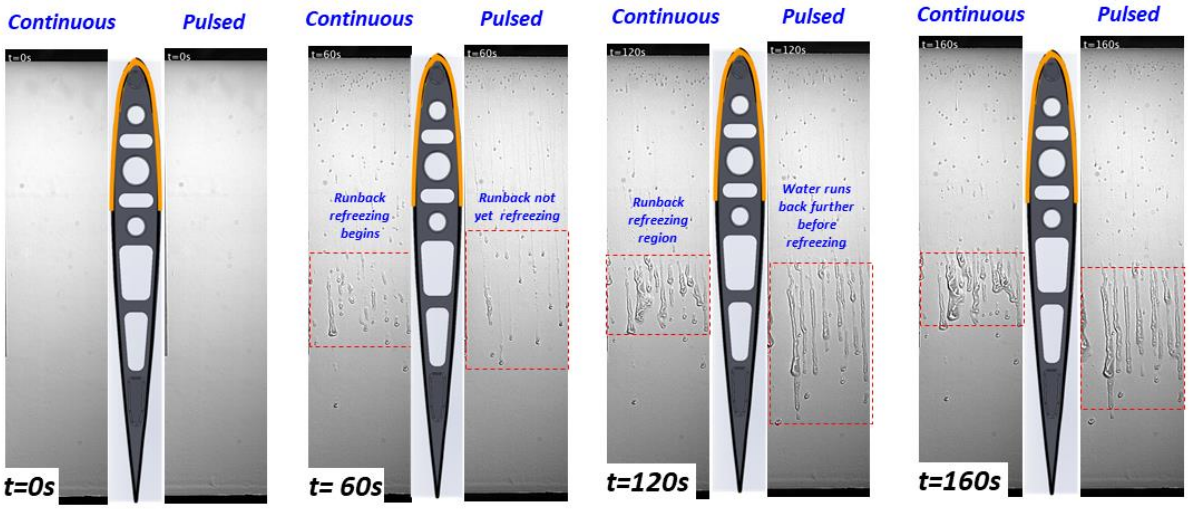

Fig. 4: Anti-icing performance for continuous and pulsed DC current at various times

While at 0 seconds, the state of the airfoil model in both the continuous and pulsed cases are identical, at 60 seconds, runback water begins to re-freeze on the continuous model, starting at approximately 50% chord. By 120 seconds, significant refreezing is observed on both the continuous and pulse-heated models. However, the region of refreezing is significantly farther rearwards on the pulse-heated model. The refreezing region extends from 42% chord to 63% chord on the continuously heated model, while the refreezing region extends from 46% chord to 83% chord on the pulse-heated model. This indicates that the pulse-heated model more effectively heats the water the water which impinges on its leading edge than the continuously heated model, and causes it to refreeze later.

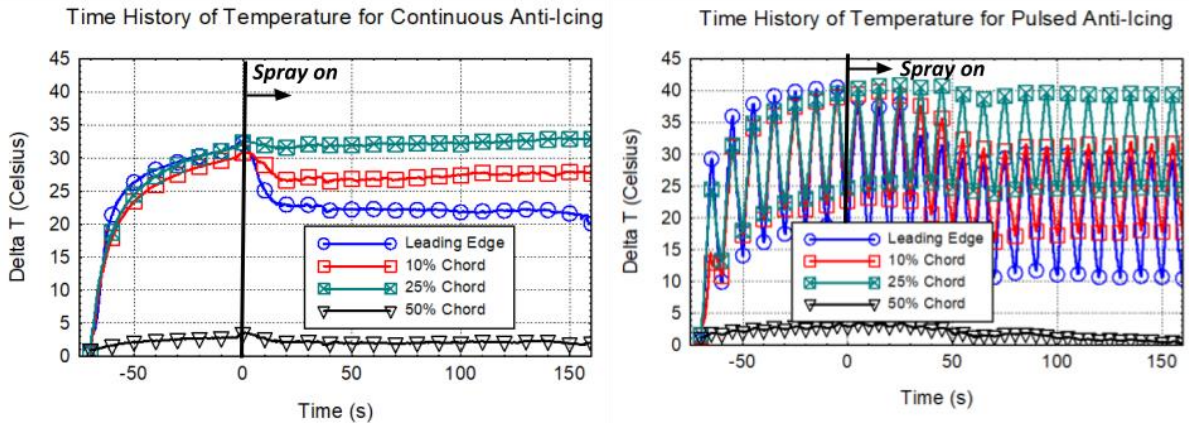

Fig. 5: Time history plots of temperature for anti-icing performance of continuous and pulsed DC current

Both the continuous and pulsed plots follow a similar trend, dropping sharply after the water spray is introduced, and then remaining relatively constant for the remainder of the test. The highest temperatures are present at 25% chord, followed by 10% chord and the leading edge. The temperature at 50% chord is nearly equal to the ambient temperature in both cases. Notably, however, the peak temperatures at each of the chord positions withing the heated region (leading edge, 10% chord, and 25% chord) are between 5 and 10 degrees Celsius higher in the pulse-heated model than on the continuously heated model. This observation supports the more effective heating of impinging water and later refreezing seen in Fig. 4., and demonstrates an advantage in anti-icing performance.

Downloaded by Iowa State University on July 18, 2024 | http://arc.aiaa.org | DOI: 10.2514/6.2023-4276

C. Continuous and Pulsed De-Icing

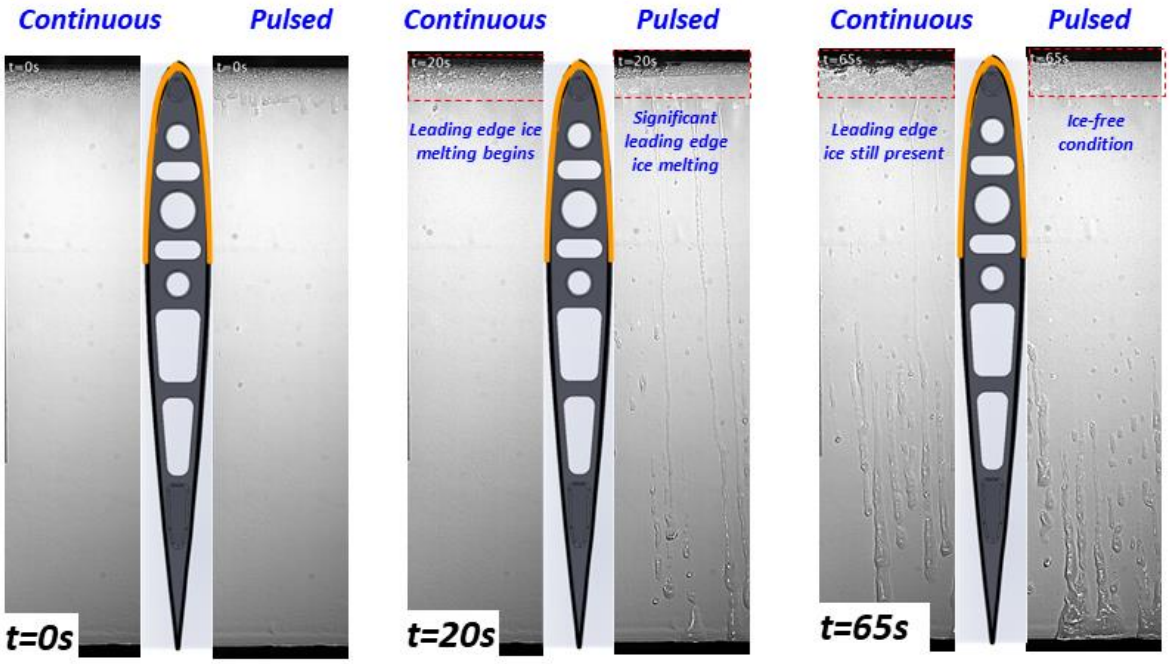

Fig. 6: De-icing performance for continuous and pulsed DC current at various times

In the de-icing test, the initial conditions were nearly identical, but at 20 seconds, a significant portion of the ice on the leading edge of the pulse-heated model has melted, while the ice accretion on the continuously heated model shows less melting. The pulsed heating case achieves an ice free condition at 65 seconds, while some ice was still present at that time in the continuous heating case. The continuously heated airfoil required 120 seconds to fully de-ice. Therefore, the pulsed heating case represents a significant improvement in de-icing performance over continuous heating. The pulse-heated model also demonstrates a further distance of runback than the continuously heated model, which indicates that the water running back subsequent to melting is at a higher temperature on the pulse-heated model than on the continuously heated model. This observation agrees with the anti-icing test detailed in Fig. 4 and Fig. 5.

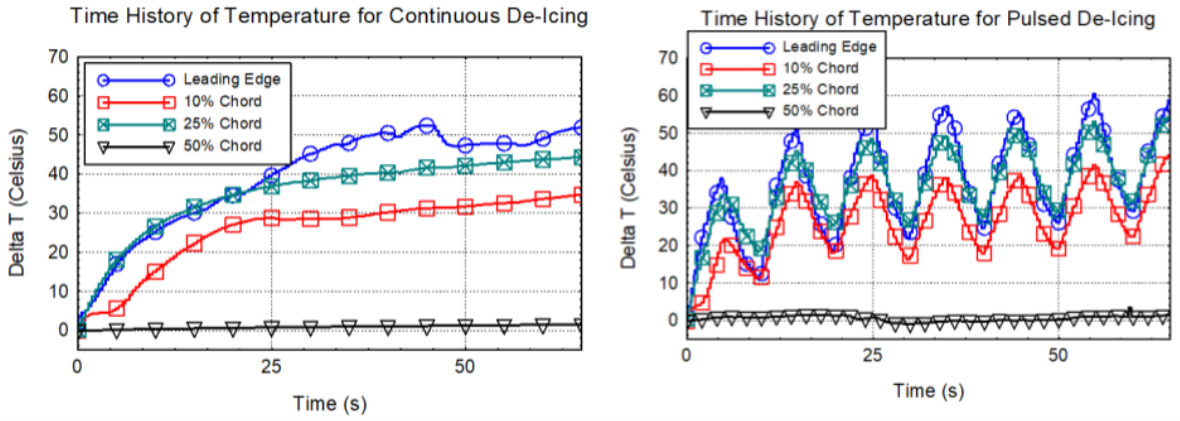

Downloaded by Iowa State University on July 18, 2024 | http://arc.aiaa.org | DOI: 10.2514/6.2023-4276

Fig. 7: Time history plots of temperature for de-icing performance of continuous and pulsed DC current

Fig. 7 demonstrates that the peak temperatures achieved by the pulse-heated model at the leading edge, 10% chord and 25% chord are approximately 10 degrees Celsius higher than the temperatures of the continuously heated model. At 60 seconds on the pulse-heated model, the temperature at 25% chord reaches 60 degrees Celsius relative to T_∞, while the continuously heated model achieves a relative temperature of 48 degrees Celsius. The considerable difference in peak temperatures corresponds with the superior de-icing performance of the pulse heated model.

V. Conclusion

In conclusion, the results of this experimental investigation demonstrate the following: At matched power, pulsed heating provides superior performance to continuous heating in both anti-icing and de-icing under the tested conditions. For anti-icing, this includes better leading edge clearing. For de-icing, this includes significantly shorter times to ice-free conditions. In this study, the power consumption of the continuous and pulsed heating were, by design, identical, allowing an advantage in performance by means of pulsed heating to be elucidated. To obtain an energy saving, in future research, the peak voltage of the pulsed waveform may be lowered to match the performance of the continuous current heating. In addition, pulsed heating may be combined with superhydrophobic or icephobic coatings to achieve full ice clearance.

Acknowledgments

References

[1] M. K. Politovich, *Aircraft Icing*, in *Encyclopedia of Atmospheric Sciences* (Elsevier, 2003), pp. 68–75. DOI:10.1016/B0-12-227090-8/00055-5.

[2] M. Zheng, Z. Guo, W. Dong, and X. Guo, *Experimental Investigation on Ice Accretion on a Rotating Aero-Engine Spinner with Hydrophobic Coating*, International Journal of Heat and Mass Transfer 136, 404 (2019). DOI:10.1016/j.ijheatmasstransfer.2019.02.104

[3] L. Tian, J. Hiller, N. Han, H. Hu, and H. Hu, *An Experimental Study on a Hybrid Anti-/De-Icing Strategy for Aero-Engine Inlet Guide Vane Icing Protection*, in *AIAA AVIATION 2022 Forum* (American Institute of Aeronautics and Astronautics, Chicago, IL & Virtual, 2022). DOI: 10.2514/6.2022-3456

[4] S. Chavan, T. Foulkes, Y. Gurumukhi, K. Boyina, K. F. Rabbi, and N. Miljkovic, *Pulse Interfacial Defrosting*, Appl. Phys. Lett. **115**, 071601 (2019). DOI: 10.1063/1.5113845

[5] H. Hu, C. Eluchie, H. Sista, H. Hu. *An Experimental Study on Anti-/de-icing Efficiency for Different Hybrid Methods.* Abstract submitted to AIAA For. Exp. 2023. (2022).

Downloaded by Iowa State University on July 18, 2024 | http://arc.aiaa.org | DOI: 10.2514/6.2023-4276